

# ***In vitro* antitumor activity of methotrexate via pH-sensitive chitosan nanoparticles**

Daniele Rubert Nogueira<sup>1</sup>, Lorena Tavano<sup>2,3</sup>, Montserrat Mitjans<sup>1,4</sup>, Lourdes Pérez<sup>2</sup>, M. Rosa Infante<sup>2</sup>, M. Pilar Vinardell<sup>1,4,\*</sup>

<sup>1</sup>*Departament de Fisiologia, Facultat de Farmàcia, Universitat de Barcelona, Av. Joan XXIII s/n, 08028, Barcelona, Spain*

<sup>2</sup>*Departamento de Tecnología Química y de Tensioactivos, IQAC, CSIC, C/Jordi Girona 18-26, 08034, Barcelona, Spain*

<sup>3</sup>*Departament of Pharmaceutical Sciences and Departament of Modeling Engineering, University of Calabria, Via P. Bucci, 87036, Arcavacata di Rende, Cozenza, Italy*

<sup>4</sup>*Unidad Asociada al CSIC, Barcelona, Spain*

Running headline: Antitumor activity of methotrexate-loaded pH-sensitive nanoparticles

\* Corresponding author. Tel.: +34 934024505; fax: +34 934035901.

*E-mail address:* mpvinardellmh@ub.edu (M. Pilar Vinardell).

## **ABSTRACT**

Nanoparticles with pH-sensitive behavior may enhance the success of chemotherapy in many cancers by efficient intracellular drug delivery. Here, we investigated the effect of a bioactive surfactant with pH-sensitive properties on the antitumor activity and intracellular behavior of methotrexate-loaded chitosan nanoparticles (MTX-CS-NPs). NPs were prepared using a modified ionotropic complexation process, in which was included the surfactant derived from N<sup>α</sup>,N<sup>ε</sup>-dioctanoyl lysine with an inorganic lithium counterion. The pH-sensitive behavior of NPs allowed accelerated release of MTX in an acidic medium, as well as membrane-lytic pH-dependent activity, which facilitated the cytosolic delivery of endocytosed materials. Moreover, our results clearly proved that MTX-CS-NPs were more active against the tumor HeLa and MCF-7 cell lines than the free drug. The feasibility of using NPs to target acidic tumor extracellular pH was also shown, as cytotoxicity against cancer cells was greater in a mildly acidic environment. Finally, the combined physicochemical and pH-sensitive properties of NPs generally allowed the entrapped drug to induce greater cell cycle arrest and apoptotic effects. Therefore, our overall results suggest that pH-sensitive MTX-CS-NPs could be potentially useful as a carrier system for tumor and intracellular drug delivery in cancer therapy.

**Keywords:** chitosan nanoparticles; methotrexate; lysine-based surfactant; intracellular drug delivery; pH-sensitivity; cytotoxicity

## 1. Introduction

Chitosan (CS) is a naturally occurring polymer that has been attracting increasing attention in pharmaceutical and biomedical applications because of its biocompatibility, biodegradability, non-toxicity, cationic properties and bioadhesive characteristics [1-3]. CS nanoparticles (NPs) have been investigated as a promising colloidal drug carrier for targeted delivery to specific sites, as well as for gene and vaccine delivery, and cancer therapy [3-5]. The ionotropic gelation technique is one of the most widely used of a variety of methods to prepare CS-NPs [1,2,6,7]. This procedure is based on reversible crosslinking by electrostatic interaction (between protonized  $-\text{NH}_3^+$  and an anion such as tripolyphosphate), instead of chemical crosslinking. It avoids the potential toxicity of reagents and the possibility of damaging the drugs, especially with biological agents [2,8].

Methotrexate (MTX) acts as an antagonist of folic acid, which is necessary for DNA synthesis, and has a therapeutic effect on many types of cancer cells that overexpress folate receptors on their surfaces [9]. MTX is currently widely used as a major chemotherapeutic agent for human malignancies such as acute lymphoblastic leukemia, malignant lymphoma, osteosarcoma, breast cancer and head and neck cancer [10]. However, its clinical efficacy is often compromised by the acquisition of resistance in cancer cells, due to cellular efflux of the molecule [11]. In this context, the encapsulation of antitumor drugs in nanoparticulated systems like polymeric NPs, which retain a higher drug concentration within the cell, might overcome the shortcomings associated with conventional drug delivery strategies [12]. MTX-loaded CS-based NPs have been developed using especially modified forms of chitosan, to improve controlled drug delivery to tumors [5,13]. A delivery system based on covalently conjugated CS-MTX has also been described, but has the drawback of using a cross-linked agent [14]. On the basis of the above studies and the need for an efficient drug carrier for cancer therapy, we decided to investigate the effect of a bioactive excipient with pH-sensitive properties on the antitumor activity and intracellular behavior of MTX-loaded CS-NPs.

Lysosomal degradation of the chemotherapeutic agent is another major hurdle for successful cancer therapy. For nanocarriers to act efficiently, they must overcome intracellular barriers, such as endosomes, and release the drugs into the cytosol before they are ultimately trafficked to lysosomes [15]. Therefore, delivery devices with bioactive excipients have been developed, which selectively release drugs or genes into the cytoplasm by sensing low pH in endosomes [16]. Bioactive compounds that could be used in nanocarriers include amino acid-based surfactants that have shown pH-responsive membrane-lytic activity [17-19]. The anionic amphiphile derived from  $N^{\alpha},N^{\epsilon}$ -dioctanoyl lysine with a lithium counterion (77KL) in particular showed pH-sensitive membrane-lytic behavior and low cytotoxicity [17]. This suggests that it may have a specific ability to destabilize the endosomal membrane in a mildly acidic environment without considerable toxic effects to the cell. Therefore, it was chosen as a bioactive excipient to be included in the pH-sensitive CS-NPs designed here as a promising carrier for the intracellular delivery of cancer drugs. In this context, CS-TPP-NPs modified by the cationic amphiphile cetyltrimethylammonium bromide are noteworthy, as they showed improved physicochemical properties, attributed to the inclusion of the surfactant [1]. The green fluorescent dye calcein and fluorescence microscopy analysis was used to monitor the capacity of the NPs to destabilize the endosomal membrane. MTX, a drug widely used in the treatment of cancer, was incorporated into CS-NPs, and the cytotoxic activity of the latter against tumor and non-tumor cell lines was assessed using *in vitro* toxicological assays.

## **2. Experimental**

### **2.1. Chemicals and reagents**

Chitosan (CS) of medium molecular weight (deacetylation degree, 75-85%; viscosity, 200-800 cP according to the manufacturer's data sheet), pentasodium tripolyphosphate (TPP), methotrexate (MTX), acridine orange (AO), ethidium bromide (EB), propidium iodide, ribonuclease A (RNase A), calcein, 2,5-diphenyl-3-(4,5-dimethyl-2-thiazolyl) tetrazolium

bromide (MTT), neutral red (NR) dye and dimethyl sulfoxide (DMSO) were obtained from Sigma-Aldrich (St. Louis, MO, USA). Dulbecco's Modified Eagle's Medium (DMEM), fetal bovine serum (FBS), phosphate buffered saline (PBS), L-glutamine solution (200 mM), trypsin-EDTA solution (170,000 U/l trypsin and 0.2 g/l EDTA) and penicillin-streptomycin solution (10,000 U/ml penicillin and 10 mg/ml streptomycin) were purchased from Lonza (Verviers, Belgium). The 75 cm<sup>2</sup> flasks and 96-well plates were obtained from TPP (Trasadingen, Switzerland). All other reagents were of analytical grade.

## 2.2. Surfactant included in the nanoparticles

An anionic amino acid-based surfactant derived from N<sup>α</sup>, N<sup>ε</sup>-dioctanoyl lysine and with an inorganic lithium counterion (77KL) was included in the NP formulation (Table 1). This surfactant was synthesized by our group as previously described [20]. The choice of 77KL as a bioactive excipient in the NP formulation was based on our previous studies, which showed its pH-sensitive membrane-disruptive activity, together with improved kinetics in the endosomal pH range and low cytotoxic potential [17,21].

## 2.3. Preparation of MTX nanoparticles

CS-NPs were prepared according to a modified version of the ionic gelation technique [6], which is based on the ionotropic complexation of CS with TPP anions. The surfactant 77KL was included in the complexation process and the NPs were prepared with a selective CS:TPP:77KL ratio of 5:1:0.5 (w/w/w).

Unloaded CS NPs (unloaded-CS-NPs) were prepared by dropwise addition of a premixed TPP and 77KL solution (both at 0.1%, w/v, with a TPP:77KL ratio equal to 1:0.5, w/w) to CS (0.1%, w/v) previously dissolved in acetic acid solution (1%, v/v). The pH of the CS final solution was adjusted to 5.5 with 1 M NaOH [7]. The NPs were formed

spontaneously and the gelation process was carried out under constant magnetic stirring (500 rpm) for 30 min at room temperature.

MTX-loaded CS NPs (MTX-CS-NPs) were prepared as follows: to a premixed TPP and 77KL solution (both at 0.1%, w/v, with a TPP:77KL ratio equal to 1:0.5, w/w), MTX was added to provide a final concentration of 0.07% (w/v) of the antitumor drug. MTX-NPs were prepared by dropwise addition of this premixed solution (TPP:77KL:MTX, with a final ratio of 1:0.5:1, w/w/w) to the previously prepared CS solution (0.1%, w/v). The NPs were formed at room temperature and dark conditions, under constant magnetic stirring (500 rpm) for 30 min. The purification of the resulting NPs was carried out by exhaustive dialysis for 4 h, using a Spectra/Por<sup>®</sup> dialysis bag of 3,500 MWCO (Spectrum Medical Industries, CA, USA).

#### 2.4. Nanoparticle characterization

The mean hydrodynamic diameter and the polydispersity index (PDI) of the NPs were determined by dynamic light scattering (DLS) using a Malvern Zetasizer ZS (Malvern Instruments, Malvern, UK). Before measurement, the NPs were appropriately diluted in both distilled water and cell culture medium with 5% FBS, and the readings were taken at 25°C immediately after preparation ( $t = 0$  h) and after 24 h incubation at 37°C ( $t = 24$  h). Each measurement was performed using at least three sets of ten runs.

The zeta potential (ZP) values of the NPs were assessed by determining electrophoretic mobility with the Malvern Zetasizer ZS equipment. The measurements were also performed in both ultrapure water and cell culture medium with 5% FBS at 25°C using at least three sets of 20 runs. ZP is a measurement of the electric charge at the surface of the particles and indicates the physical stability of colloidal systems.

The morphology and size of the NPs were analyzed by transmission electron microscopy (TEM). A droplet (5  $\mu$ l) of the NPs dispersed in distilled water was placed on a carbon-coated copper grid to form a thin liquid film, and the negative staining of samples was

obtained with a 2% (w/v) solution of uranyl acetate. The images were obtained with a Jeol JEM-1010 electron microscope (Jeol Ltd., Tokyo, Japan) operating at an acceleration voltage of 80 kV.

## 2.5. Drug entrapment efficiency

The drug association efficiency was determined using the dialysis technique for separating the non-encapsulated drug from the NPs. Five milliliters of drug-loaded NPs was dropped into a dialysis bag (Spectra/Por<sup>®</sup>, 3,500 MWCO, Spectrum Medical Industries, CA, USA), the free drug was dialyzed for 60 min each time and the dialysis was completed when no drug was detectable in the recipient solution. The percentage of encapsulation efficiency (E%) of MTX in the NPs was measured using UV spectrophotometry (306 nm, UV-160A spectrophotometer, Shimadzu, Kyoto, Japan) and calculated as follows [22]:

$$E\% = 100 \times (ND - D) / ND \quad (1)$$

where ND and D are the drug concentrations before and after the dialysis, respectively. The E% value was the mean of three NP batches.

## 2.6. *In vitro* release study

*In vitro* release assessments from MTX-loaded CS NPs were carried out for 24 h in phosphate buffered saline (PBS) at pH 7.4, 6.5 and 5.4. An aliquot of NPs (100 µg/ml) was placed in a dialysis bag (Spectra/Por<sup>®</sup>, 3,500 MWCO, Spectrum Medical Industries, CA, USA) and suspended in 15 ml of PBS at 37°C under gentle magnetic stirring (100 rpm). At scheduled times, 2 ml of medium was withdrawn and replaced with an equal volume of fresh medium. The amount of MTX released was estimated by UV spectrophotometry (306 nm, UV-160A spectrophotometer, Shimadzu, Kyoto, Japan). All of the experimental procedure was performed in triplicate. The release of the free drug was also investigated in the same

way. The cumulative release percentage (CR%) of MTX at each time point was determined using the following equation:

$$\text{CR}\% = (M_t / M_i) \times 100 \quad (2)$$

where  $M_i$  and  $M_t$  are the initial amount of drug encapsulated in the NPs and the amount of drug released at the time  $t$ , respectively.

## 2.7. Cell cultures and treatments

The tumor cell lines HeLa (human epithelial cervical cancer) and MCF-7 (human breast cancer), and the non-tumor cell line HaCaT (spontaneously immortalized human keratinocytes) were grown in DMEM medium (4.5 g/l glucose) supplemented by 10% (v/v) FBS, 2 mM L-glutamine, 100 U/ml penicillin and 100  $\mu\text{g/ml}$  streptomycin at 37°C, 5%  $\text{CO}_2$ . These cells were routinely cultured in 75  $\text{cm}^2$  culture flasks and were trypsinized using trypsin-EDTA when the cells reached approximately 80% confluence. All cell lines were obtained from Eucellbank (Universitat de Barcelona, Spain).

HeLa ( $5 \times 10^4$  cells/ml), MCF-7 ( $1 \times 10^5$  cells/ml) and HaCaT ( $1 \times 10^5$  cells/ml) cells were seeded into the 60 central wells of 96-well cell culture plates in 100  $\mu\text{l}$  of complete culture medium. Cells were incubated for 24 h under 5%  $\text{CO}_2$  at 37°C and the medium was then replaced with 100  $\mu\text{l}$  of fresh medium supplemented by 5% (v/v) FBS containing the treatments. Unloaded-CS-NPs were assayed in the 3.9-500  $\mu\text{g/ml}$  concentration range, whereas MTX-CS-NPs and free MTX were assessed in the 0.001-50  $\mu\text{g/ml}$  concentration range. The concentration of unloaded-CS-NPs was based on their total composition, and the higher concentration range tested was attributed to their low cytotoxic potential. In contrast, the concentration of MTX-CS-NPs was based on the total amount of MTX encapsulated in the NPs, so that the results could be compared with those obtained using free MTX. Each concentration was tested in triplicate and control cells were exposed to medium with 5% (v/v)

FBS only. The cell lines were exposed for 4, 24 or 48 h to each treatment, and their viability was assessed by three different endpoints, as described below.

To assess the pH-dependent cytotoxicity of NPs and free MTX, we also exposed the cells to treatment at pH 6.6, which mimicks the acidic extracellular pH of tumors (pH<sub>e</sub>) [23]. DMEM 5% FBS was mixed with 1 M HEPES buffer pH 6.2 at a ratio of 5:1, and the resulting mixture, with an experimental pH of 6.6, was applied during the incubation of the NPs or free MTX (at the same concentration range as that described above) with HeLa or MCF-7 cells for 4 or 24 h.

## 2.8. Cytotoxicity assays – antitumor activity of MTX

The MTT assay is based on the protocol first described by Mossmann [24]. It is a measurement of cell metabolic activity, and correlates quite well with cell proliferation [25]. The assay was performed as previously described [26]. Cell viability was calculated as the percentage of tetrazolium salt reduction by viable cells in each sample and the values were normalized by the untreated cell control (cells with medium only).

The NRU assay is based on the protocol described by Borenfreund and Puerner [27], and reflects the functionality of the lysosomes and plasma membrane [28]. The assay was performed following the previously described protocol [26]. The effect of each treatment was calculated as the percentage of uptake of NR dye by lysosomes against the untreated cell control (cells with medium only).

LDH leakage was evaluated to determine the integrity of the plasma membrane using a commercially available kit (Takara Bio Inc, Otsu, Japan), in line with the instructions provided by the manufacturer. This assay quantifies cytotoxicity by measuring LDH released from dead or plasma membrane-damaged cells into the supernatant [29]. Absorbance was measured in a microplate reader (Sunrise<sup>TM</sup>, Tecan, Switzerland) at 492 nm, with 620 nm set

as the reference wavelength. The results are expressed as a percentage of control, with 1% Triton-X used as a positive control.

To determine whether the NPs interacted with the viability assays, UV/Visible absorbance measurements were carried out [30]. Unloaded-CS-NPs at 500 µg/ml and MTX-CS-NPs at 50 µg/ml were suspended in DMEM medium (without FBS and phenol red) containing MTT (0.5 mg/ml) or NR (50 µg/ml) dyes, and the occurrence of dye interference was assessed following the previously described procedure [26].

## 2.9. Apoptosis

NP-induced apoptosis in HeLa and MCF-7 cells was quantified using acridine orange/ethidium bromide (AO/EB) double staining, according to standard procedure [31] and using a fluorescence microscope. Briefly, cells were seeded ( $5 \times 10^4$  or  $1 \times 10^5$  cells/ml, for HeLa and MCF-7, respectively) in 24-well plates and treated with 1, 10 or 50 µg/ml of MTX-CS-NPs or free MTX. After 24 h incubation, the cells were trypsinized and centrifuged at 1200 rpm for 5 min. Then, fluorescent dyes AO (0.5 µg/ml) and BE (10 µg/ml) were added to the cellular pellet. Freshly stained cell suspension was dropped on a glass slide and covered by a cover slip. Slides were observed with an Olympus BX41 fluorescence microscope equipped with a UV-mercury lamp (100W Ushio Olympus) and a U-N51004v2- FITC/TRITC type filter set (FITC: BP480-495, DM500-545, BA515-535 and TRITC: BP550-570, DM575-, BA590-621). Images were digitized on a computer through a video camera (Olympus digital camera XC50) and were analyzed with an image processor (Olympus cell^B Image Acquisition Software). The percentage of viable, apoptotic and necrotic cells was determined in at least 100 cells.

## 2.10. Cell cycle analysis by flow cytometry

HeLa and MCF-7 tumor cells were cultured in 60 mm petri dishes for 24 h at a density of  $5 \times 10^4$  or  $1 \times 10^5$  cells/ml, respectively, and then treated with 1, 10 or 50  $\mu\text{g/ml}$  of MTX-CS-NPs or free MTX. After 24 h treatment, the cells were harvested by trypsinization, washed in cold PBS, fixed in ice-cold 70% ethanol and kept at  $-20^\circ\text{C}$ . Fixed cells were centrifuged, resuspended in DNA extraction buffer (0.2 M  $\text{Na}_2\text{PO}_4$  and 0.1 M citric acid, pH 7.8) and incubated for 30 min at  $37^\circ\text{C}$ . Then, the cells were stained with staining solution (20  $\mu\text{g/ml}$  propidium iodide, 200  $\mu\text{g/ml}$  RNase A and Triton X-100 in PBS). The samples were kept in dark conditions for 1 h and measured with the Beckman Coulter ADC Epics XL flow cytometer (Beckman Coulter, FL, USA) (15,000 events were acquired for each sample). The data obtained were processed for cell cycle analysis with Multicycle<sup>®</sup> software. The amount of propidium iodide intercalating to DNA was used as the parameter to determine the cell cycle distribution phases.

#### 2.11. Lysosomal membrane integrity

Lysosomal membrane stability was assessed using the acridine orange (AO) relocation technique. AO is a lysosomotropic base ( $\text{pK}_a = 10.3$ ) that produces a red fluorescent emission when accumulated in acidic lysosomes. Disruption of the lysosomal membrane can be assessed by measuring the change in intracellular AO fluorescence (i.e., loss of the lysosomal red signal and gain of cytoplasmic green) [32]. HeLa and MCF-7 cells were exposed to MTX-CS-NPs or free MTX (final concentrations of 1, 10 and 50  $\mu\text{g/ml}$ ) for 24 h. Then, the cells were trypsinized, centrifuged at 1200 rpm for 5 min, and 2  $\mu\text{g/ml}$  AO was added to the cellular pellet. Freshly stained cell suspension was dropped on a glass slide and covered by a cover slip. Slides were observed on an Olympus BX41 fluorescent microscope, as described in Section 2.9.

#### 2.12. Hemocompatibility studies

Erythrocytes were isolated from rat blood, which was obtained from anesthetized animals by cardiac puncture and drawn into tubes containing EDTA. The procedure was approved by the institutional ethics committee on animal experimentation. The hemolysis assay was performed following the previously described procedure [17]. Twenty-five microliter aliquots of erythrocyte suspension were exposed to unloaded-CS-NPs at concentrations of 100, 250 and 500  $\mu\text{g/ml}$ , and to MTX-CS-NPs or free MTX at concentrations of 10, 25 and 50  $\mu\text{g/ml}$ . The samples were incubated at room temperature for 10 minutes or 1 h. For the studies of erythrocyte agglutination, 10  $\mu\text{l}$  of each sample was subjected to a hemolysis assay for 1 h (500  $\mu\text{g/ml}$  of unloaded-CS-NPs and 50  $\mu\text{g/ml}$  of MTX-CS-NPs), placed on a glass slide, covered by a cover slip and analyzed by a phase contrast microscope (Olympus BX41, Olympus, Japan).

### 2.13. pH-dependent membrane-lytic activity of nanoparticles

#### 2.13.1. Hemolysis assay as a model for the endosomal membrane

The pH-dependent membrane-lytic activity of the NPs was assessed using erythrocytes as a model of the endosomal membrane [33,34]. Increasing concentrations of unloaded-CS-NPs and MTX-CS-NPs were added to erythrocytes suspended in PBS buffer of pH 7.4, 6.5 or 5.4. The extent and kinetics of hemolysis were assessed as reported earlier [17].

#### 2.13.2. Cell uptake studies - intracellular release of calcein

Calcein, a membrane-impermeant fluorophore, was used as a model drug molecule and tracer to monitor the stability of endosomes following vesicle uptake [35]. HeLa cells were plated ( $5 \times 10^4$  cells/ml) in 24-well plates on round cover glasses (Marlenfeld GmbH & Co.KG, Lauda-Könlghshofen, Germany) and incubated overnight at 37°C under 5%  $\text{CO}_2$ . Then, calcein (1 mg/ml) was added to the cells with or without (control cells) 250 or 500  $\mu\text{g/ml}$  of unloaded-CS-NPs, or 25 or 50  $\mu\text{g/ml}$  of MTX-CS-NPs in DMEM medium without FBS and

phenol red. After 1 h incubation at 37°C, the cells were washed four times with PBS and incubated in complete medium for 3 h to allow intracellular trafficking. The cells were then washed with PBS and fixed with 4% (v/v) formaldehyde in PBS (pH 7.4) for 15 min at room temperature. Each individual cover glasses was mounted on clean glass slides with Prolong® Gold antifade reagent (Invitrogen) and analyzed on an Olympus BX41 fluorescence microscope equipped with a MNIBA3 filter set type (470-495 nm excitation, 510-550 nm emission and 505 nm dichromatic mirror). Images were digitized and analyzed as described in Section 2.9.

#### 2.14. Statistical analysis

All *in vitro* experiments were performed at least three times, using three replicate samples for each formulation concentration tested. The cytotoxicity of each formulation was expressed in terms of its IC<sub>50</sub> (concentration causing 50% death of the cell population), calculated from concentration-response curves. Results are expressed as mean ± standard error of the mean (SE). Statistical analyses were performed using the Student's *t* test or one-way analysis of variance (ANOVA) to determine the differences between the datasets, followed by Tukey's or Dunnett's *post-hoc* test for multiple comparisons using SPSS® software (SPSS Inc., Chicago, IL, USA).  $p < 0.05$  and  $p < 0.005$  were considered significant.

### 3. Results

#### 3.1. Characterization of nanoparticles

Unloaded- and MTX-loaded NPs were characterized by DLS and TEM. Firstly, we assessed the effects of the dispersion medium (distilled water or culture medium), temperature and exposure time on NP hydrodynamic size. DLS measurements showed that fresh prepared ( $t = 0$ ) unloaded-CS-NPs and MTX-CS-NPs dispersed in distilled water had an average hydrodynamic size of 350 nm and 301 nm, respectively (Table 2). After 24 h incubation ( $t =$

24) at 37°C, the NPs showed a slight size increase. In contrast, when the NPs were dispersed in the cell culture medium (DMEM with 5% FBS), the size increase was moderate by 0 h (579 nm and 483 nm for unloaded-CS-NPs and MTX-CS-NPs, respectively), which indicates that NP agglomeration took place. After 24 h incubation under cell culture conditions, the unloaded-CS-NPs presented a bimodal size distribution, with particles smaller (108 nm) and larger (723 nm) than those obtained at  $t = 0$ . However, all the MTX-CS-NPs had a hydrodynamic size that was three times smaller (147 nm) after 24 h incubation in cell culture medium. PDI values below 0.3 were obtained in distilled water at both  $t = 0$  and  $t = 24$ , which indicates that the NP population was relatively homogenous in size. In contrast, significantly higher PDI values ( $> 0.4$ ) were found for the NPs dispersed in the cell culture medium. The NPs dispersed in water showed positive ZP values ( $\sim 30$  mV), whereas almost neutral values were obtained in cell culture medium.

A TEM analysis was also performed to assess NP morphology and size (Table 2). The results showed that at  $t = 0$  both unloaded-CS-NPs and MTX-CS-NPs dispersed in water had a roughly spherical shape and were much smaller ( $\sim 20$ -140 nm and  $\sim 20$ -60 nm, respectively) than the hydrodynamic size determined by DLS (350 and 301 nm, respectively). Finally, the entrapment efficiency achieved for NPs was found to be  $63.41 \pm 0.65\%$  for MTX. This high incorporation capacity in the designed formulation is probably related to the chemical nature of the drug and to its interactions with the NP structure at the pH value of the experimental conditions.

### 3.2. *In vitro* release study

The pH-dependent cumulative amount of MTX released from the MTX-CS-NPs is shown in Fig. 1. A control experiment using free MTX was also carried out under similar conditions and complete diffusion across the dialysis membrane was found to occur within 3 h. The release of MTX from NPs at physiological pH showed an initial burst release of 18%

after 1 h, whereas about 75% and 100% was released after 8 h and 24 h, respectively. The initial MTX burst release at pH 6.5 was almost the same as at pH 7.4 (~18%), but greater release was achieved at each subsequent time point. In contrast, significantly faster ( $p < 0.05$ ) drug release was obtained at pH 5.4: approximately 42% of the MTX was released from the NPs after 1 h, while total drug release was reached after only 6 h.

### 3.3. *In vitro* cytotoxicity assessments

#### 3.3.1. Cell viability studies – antitumor activity

The MTT and NR dye interactions with NPs were studied to test the suitability of MTT and NRU viability assays for the cytotoxicity evaluation of CS-NPs. Our results showed slight interference of the NPs with the viability dyes. The NPs, especially the unloaded-CS-NPs, induced a slight increase in the MTT and NR absorbance values at 550 nm. These data were proved by the UV-vis measurements (data not shown). However, the interferences observed did not result in a further increase in cell viability with increasing NP concentration, which demonstrated that these interactions between NPs and viability dyes were not significant, and also proved that the viability endpoints are suitable for the intended purpose.

The cytotoxicity studies of unloaded-CS-NPs, MTX-CS-NPs and free MTX were performed using tumor (HeLa and MCF-7) and non-tumor (HaCaT) cell lines. Our results clearly proved that the activity of MTX-CS-NPs against the tumor cells was greater than that of the free drug (Fig. 2 and Table 3). The MTT and NRU endpoints showed moderate cytotoxic effects of free MTX (> 60% of viability), whereas MTX encapsulated in the NPs significantly reduced the cell growth by up to 17% and 33% of viability in HeLa and MCF-7 cells, respectively (Fig. 2A). The MCF-7 cell line displayed higher resistance than the HeLa cells to both free MTX and MTX-CS-NPs. The non-tumor HaCaT cell line was much less sensitive to the antiproliferative and toxic effects of the MTX-CS-NPs (Fig. 2), with viabilities higher than 56% or 85% as measured by the MTT and NRU assays, respectively. Likewise,

the free MTX showed cytotoxicity to the HaCaT cells of less than 20%. Furthermore, the NPs affected cell viability in a time-dependent manner when they were added to the cells in the concentration range of 0.001-50  $\mu\text{g/ml}$  for up to 48 h (Fig. 3A). The free MTX displayed similar cytotoxic behavior, but to a less significant extent. Table 3 shows the  $\text{IC}_{50}$  values (determined by the MTT assay) of the MTX-CS-NPs and free drug tested at 4, 24 and 48 h. Unloaded-CS-NPs showed low cytotoxic effects against all tested cell lines and displayed, in general,  $\text{IC}_{50}$  values  $> 500 \mu\text{g/ml}$  and at least 60% of cell viability (Table 3). Finally, as determined by the LDH assay, unloaded-CS-NPs, MTX-CS-NPs and free MTX did not affect the plasma membrane integrity of the three cell lines. Viability values above 90% were obtained in all the conditions tested.

Fig. 3B shows the effect of the medium's pH during cell treatment on the cytotoxic responses of free MTX and MTX-CS-NPs in the tumor cell lines. Free MTX did not show any change in its cytotoxic activity on HeLa and MCF-7 cells when it was incubated under mildly acidic conditions (pH 6.6) for 4 and 24 h. In contrast, the higher concentrations of MTX-CS-NPs displayed significantly higher cytotoxicity ( $p < 0.005$ ) to both tumor cell lines after 4 h incubation at pH 6.6. The  $\text{IC}_{50}$  values decreased from  $> 50$  to 21.86  $\mu\text{g/ml}$  and  $> 50$  to 33.09  $\mu\text{g/ml}$  in HeLa and MCF-7 cells, respectively. After 24 h incubation, the cytotoxic profile of the NPs was similar at both pH in HeLa cells, whereas in MCF-7 cells, the concentration of 10  $\mu\text{g/ml}$  showed significantly higher cytotoxicity at pH 6.6. The cytotoxic profile of unloaded-CS-NPs did not change significantly when incubated at pH 6.6 (data not shown).

### 3.3.2. Apoptosis

In order to determine whether the initial cell death observed in HeLa and MCF-7 tumor cells exposed to free MTX and MTX-CS-NPs could be due to apoptosis, AO/EB staining was carried out and the samples were analyzed under a fluorescence microscope. Fig. 4 reveals a significant increase ( $p < 0.05$  or  $p < 0.005$ ) in the number of apoptotic cells in both cell lines

following treatment with free MTX and MTX-CS-NPs. Furthermore, a greater increase in the fraction of apoptotic cells was induced by MTX-CS-NPs than by free MTX, especially in HeLa cells. The effects were dose-dependent for both MTX-CS-NPs and free MTX. The most significant effects were observed with the treatments that were also the most cytotoxic in all the viability assays. A slight to moderate increase was observed in the number of cells undergoing late apoptosis or necrosis, but these results did not differ significantly from those of the control cells. The untreated HeLa and MCF-7 cells were observed with a green intact nuclear structure (Fig. 4c and f, respectively), while after free MTX or MTX-CS-NP treatments we observed cells showing blebbing and nuclear margination (e.g. in Fig. 4d), chromatin condensation (e.g. in Fig. 4e) (early and moderate apoptosis), orange nuclei with normal chromatin distribution (necrosis) (e.g. in Fig. 4g), as well as apoptotic body separation and a reddish-orange color (late apoptosis) (e.g. in Fig. 4h).

### 3.3.3. Cell cycle analysis

A flow cytometric analysis was performed to clarify the influence of MTX-CS-NPs on cell-cycle distribution in comparison with the free drug, and in addition to the cell viability studies. These experiments showed significant ( $p < 0.05$  or  $p < 0.005$ ) suppression of the G1/G0 and G2/M phases with cell cycle arrest in the S phase in both HeLa and MCF-7 cancer cells (Fig. 5). In HeLa cells, this effect was more pronounced after the free MTX treatment. In contrast, the MTX-CS-NPs induced greater accumulation of cells in the S phase in MCF-7 after 24 h exposure. The distinct cell cycle arrest phase observed in cells treated with free MTX or MTX-CS-NPs might be due to the different consequences of unloaded or nanocarrier-loaded MTX in cancer cells. Moreover, a significant increase in the cell population was observed in the sub-G1 phase after treatment with MTX-CS-NPs, which is indicative of apoptotic cells. This corroborates the apoptosis experiments using AO/EB staining.

### 3.3.4. Lysosomal membrane integrity

The ability of free MTX and MTX-CS-NPs to induce lysosomal membrane permeabilization (LMP) was assessed using the AO relocation assay (Fig. 6). In control HeLa and MCF-7 cells, the lysosomes (red-orange granules) can be clearly seen as strong granular AO staining. MCF-7 cells treated with both MTX and MTX-CS-NPs showed little or no LMP by microscopic observation, whereas HeLa cells showed an increased LMP effect induced by 50  $\mu\text{g/ml}$  MTX-CS-NPs, as evidenced by the release of lysosomal contents into the cytoplasm (a reduction in red fluorescence).

### 3.4. Hemocompatibility studies

The hemocompatibility of the NPs and free MTX was studied by hemolysis experiments (Fig. 7A). The release of hemoglobin was used to quantify their erythrocyte-damaging properties. The unloaded-CS-NPs were non-hemolytic (less than 5%) after 10 min incubation and showed slight hemolysis after 1 h incubation (about 10% at the highest concentration). In contrast, MTX-CS-NPs at 50  $\mu\text{g/ml}$  induced significantly higher hemolysis (> 70%) after both 10 and 60 min incubation. The free MTX was non-hemolytic in all the conditions. In addition, neither unloaded-CS-NPs nor MTX-CS-NPs induced agglutination of erythrocytes after 1 h of treatment with the lowest concentrations tested (100 and 250  $\mu\text{g/ml}$  or 10 and 25  $\mu\text{g/ml}$ , respectively) (data not shown). In contrast, significant agglutination was induced by 500  $\mu\text{g/ml}$  of unloaded-CS-NPs and 50  $\mu\text{g/ml}$  of MTX-CS-NPs (Fig. 7B).

### 3.5. pH-dependent membrane-lytic activity of nanoparticles

#### 3.5.1. Hemolysis assay as a model for the endosomal membrane

Fig. 8A shows the membrane-lytic activity of the NPs as a function of concentration with varying pH and incubation time. Negligible membrane lysis was induced by unloaded-CS-NPs after 10 min incubation at physiological pH, while 60 min incubation prompted at

most 11% of hemolysis. Interestingly, MTX-CS-NPs at 50  $\mu\text{g/ml}$  induced 70.5% and 94.5% of membrane lysis after 10 and 60 min incubation, respectively. As the pH decreased to 6.5 or 5.4, the membrane-lytic activity of the unloaded-CS-NPs increased significantly ( $p < 0.05$ ) in a dose-dependent manner. The unloaded-CS-NPs reached a maximum hemolysis of 61.2% and 83.5% after 60 min of incubation at pH 6.5 and 5.4, and were 5.5- and 7.6-fold more hemolytic than at pH 7.4, respectively. MTX-CS-NPs showed higher membrane lysis in an acidic environment and were also more active than the unloaded-CS-NPs. MTX-CS-NPs at 25  $\mu\text{g/ml}$  already induced 12.9% and 43.4% of hemolysis after 60 min incubation at pH 6.5 and 5.4, respectively, and were 4.8- and 16.1-fold more hemolytic than at pH 7.4. At 50  $\mu\text{g/ml}$ , the membrane-lytic activity did not differ significantly from that at pH 7.4. Finally, unloaded-CS-NPs without 77KL were prepared to prove that the pH-sensitive membrane-lytic activity of the NPs could be attributed to the surfactant. These NPs showed at most 3.8%, 11.6% and 15.5% of hemolysis at pH 7.4, 6.5 and 5.4, respectively. The hemolysis of free MTX was also assessed at pH 7.4, 6.5 and 5.4, but no membrane lysis was obtained in any of the conditions (data not shown).

### 3.5.2. Calcein uptake and endosomal stability

The ability of the NPs to release endocytosed materials into the cell cytoplasm was examined by fluorescence microscopy, following the uptake of calcein and NPs into HeLa cells. As shown in Fig. 8B, cells treated with calcein alone (control cells) showed a bright punctate distribution of fluorescence, which is consistent with constitutive endocytosis of the external medium. When the cells were co-incubated with calcein and unloaded-CS-NPs or MTX-CS-NPs, diffuse green fluorescence staining was observed in the cytoplasm, which indicates destabilization of the endosomal membrane and release of calcein to the cell cytosol. These results corroborated the hemolysis experiments, in which the NPs showed increased membrane-lytic activity in the pH range characteristic of endosomal compartments.

#### 4. Discussion

The ionic gelation method was chosen to form the NPs because of the ability of CS to gel spontaneously on contact with multivalent polyanions. To form ionic crosslinks with TPP and 77KL, the pH of CS solution was set at 5.5, because at this pH the formation of smaller NPs with higher ZP value was reported [7]. In addition, at pH 5.5, about 90% of the amino groups of CS ( $pK_a = 6.5$ ) are protonated [36], which ensures that the crosslinking process takes place to form CS-TPP-NPs. Finally, a pH value of 5.5 would ionize ~50% of the carboxylic groups of MTX ( $pK_a = 4.8$  and  $5.5$ ), which allows attractive electrostatic interactions between the negatively charged drug molecules and positively charged CS molecules [6]. Therefore, during the process of incorporating the drug into the NPs, we can assume that the MTX molecules are both adsorbed at the particle surface [37] and entrapped/embedded in the CS nano-matrix by hydrogen bonding and hydrophobic forces [6].

The NP hydrodynamic size characterization in water using DLS showed that only a small increase in mean diameter was observed after 24 h, which means that the incubation time and temperature of the cell culture experiments did not directly affect the stability of the NPs, and that the dispersion medium plays a key role in their aggregation behavior. When dispersed in cell culture medium and maintained in the conditions of the cytotoxicity assays, both unloaded-CS-NPs and MTX-CS-NPs displayed unexpected behavior. The increase in measured particle size at  $t = 0$  in protein-containing medium may be due to protein coating of the particles and aggregation [7,28]. At the pH of the cell culture medium ( $\sim 7.4$ ), there is a considerable reduction in the degree of protonation at the NPs surface (confirmed by the ZP values), which decreases electrostatic repulsion between the particles and, thereby, increases the probability of particle aggregation. However, the decreasing protonation state of the CS molecule in the particle surface might lead to desorption of the superficial molecules, due to reduced ionic interaction with both TPP and 77KL. This process probably has a slow equilibration, which may justify the shaping of smaller NPs after 24 h incubation in the cell

culture medium. The MTX-CS-NPs showed a slight reduction in the ZP value that may be due to the decreased number of free positive groups of CS in the NP surface, which electrostatically attached to the MTX molecules. The TEM experiments displayed NPs with a much smaller diameter than the hydrodynamic size measured by DLS, which could be due to the resolution limitation of DLS [38], to the swelling of the NPs in the presence of water [4] or even to the fact that DLS gives the mean hydrodynamic diameter of the particle core surrounded by the solvation layers, whereas TEM gives the diameter of the particles alone in the dry state [39]. NPs loaded with MTX were even smaller than unloaded-CS-NPs (as also demonstrated by DLS), which suggests that the drug increased the degree of NP compaction. Moreover, in the TEM images we can see some other material that is not condensed in the structure of the NPs, which might be unreacted polymer chains that are not involved in NP formation.

It was shown that the cumulative release rates of MTX from NPs were effectively slower than those of the free drug solution. The observed initial burst release of MTX from the NPs might be due to drug molecules that were loosely incorporated into them, e.g., by electrostatic interaction between the positively charged amino groups of CS in the particle surface and the ionized carboxyl groups of MTX. At physiological pH, we obtained a relatively slow release up to 24 h, which could be attributed to drug diffusion and the swelling/degradation of the polymer [40]. In contrast, the release rate was accelerated by decreasing pH, which confirms the pH-dependent release pattern of this nanoarchitecture. The slightly increased release at pH 6.5 might mean that anticancer drug delivery is triggered at tumor extracellular pH<sub>e</sub> (a pH range from 6.5 to 7.2) [23] or early endosomal compartment. Moreover, the MTX release from NPs was significantly increased at pH 5.4, which supports the idea of effectively increased intracellular drug delivery through the late endosomes. The triggered release of payload under acidic conditions might be attributed to the pH-dependent activity of 77KL [17]. The ionization of 77KL (pK<sub>a</sub> = 6.2) tends to decrease under acidic

conditions, which might contribute to destabilizing the NP structure, due to the reduced amount of available anionic groups that interact electrostatically with the positive amino groups of CS. Finally, high release in an acidic environment might be favored by the lower degree of MTX ionization under this condition, which would decrease the electrostatic interaction of the drug with the positively charged NP surface. The development of a switching carrier in release kinetics, from slow release while circulating to rapid release kinetics once target sites have been reached, is of great importance to avoid the multidrug resistance (MDR) of initially sensitive tumor cells caused by slow release at the site of action [23].

*In vitro* model systems provide a rapid and effective means to assess NPs for a number of toxicological endpoints and mechanism-driven responses. Here, we showed the relative selectivity of the NPs for cancer cells, as the cytotoxic effects of MTX-CS-NPs were significantly lower in the non-tumor control cells (HaCaT). These findings might be related to distinct cell uptake depending on the cell nature or cell proliferative status. Moreover, we clearly showed that the MTX-CS-NPs had greater antitumor effects *in vitro* against the cancer cells than the free MTX. The low antiproliferative effect of the native drug obtained in our study is very well correlated with the duration of its intracellular retention. Free MTX is found to be pumped off the cell cytosol by P-glycoprotein, which participates in the development of resistance to antifolates [41]. Moreover, the availability of free MTX at its intracellular site of action depends on a passive diffusion mechanism, which can be limited by the high ionization state of MTX at physiological pH. In contrast, the obviously enhanced cytotoxicity of MTX via the nano-sized particles means that there was a significant reverse effect of drug resistance. NPs could reduce the MDR that characterizes many anticancer drugs by a mechanism of cell internalization of the drug by endocytosis [42], by lowering drug efflux from the cells [43] and/or by allowing pH-dependent drug release from the endosomes to cell cytosol [44]. As demonstrated in Section 3.5, the pH-sensitivity of NPs allowed their rapid escape from the endosomal compartment, which may enhance their therapeutic efficiency

compared to the native drug. MTT was the most sensitive viability assay for detecting the cytotoxic effects of the NPs, regardless of the cell line. This implies that although NPs primarily exerted toxicity on the mitochondrial compartment after cellular internalization, the plasma membrane remained intact. This finding could be related to the mechanism of action of MTX. MTX is a potent inhibitor of the enzyme dihydrofolate reductase, which plays a key role in the synthesis of DNA precursors and cell growth [10]. Therefore, MTX is a chemotherapeutic agent that mainly inhibits cell proliferation, which justifies the lack of LDH release to the cell cytosol due to membrane rupture (late stage of cell death). We also showed that unloaded-CS-NPs reduced cell viability, especially in HeLa cells. This is most likely due to the combined effect of the free amines of the polymer at the NP surface and the cytotoxic potential of the surfactant by itself. Finally, although our overall results were in line with a previous report [10] and showed that MCF-7 cells displayed resistance to MTX, we also proved the greater activity of MTX-CS-NPs against this cell line.

The cytotoxic activity of pH-sensitive NPs was also investigated to test their feasibility in targeting acidic tumor extracellular pH<sub>e</sub>. Although free MTX had no enhanced effect in an acidic environment, the MTX loaded into the NPs showed pronounced cytotoxicity at low pH, which might be attributed to the accelerated release of MTX triggered by pH. Moreover, the increased cytotoxicity at pH 6.6 may be due to the combined effect of increased protonation of 77KL and CS groups on the NP surface at tumor pH, which increases binding to the cell membrane, leading to greater internalization and, thus, greater NP cytotoxicity. These findings support the idea that the MTX-CS-NPs truly discriminate the small difference between the physiological and tumor pH<sub>e</sub> by destabilization and the release rate [23].

After we had shown that MTX-CS-NPs exerted cytotoxic effects on the proliferation of cancer cells in a typically dose-dependent manner, we examined whether the induction of apoptosis, LMP or alterations in the normal cell cycle were the possible molecular mechanisms involved in the antitumor activity of NPs in comparison to the free drug.

Although the treatment of cancer cells with free MTX significantly inhibited the cell cycle in the S-phase, these cells were essentially more resistant to free MTX-induced apoptosis. In contrast, MTX-CS-NPs induced more significant signs of apoptosis, increased the reduction in cell proliferation and also arrested the cell cycle in the S-phase. Altogether, these data indicated that free MTX acted mainly as a cytostatic drug on HeLa and MCF-7 cancer cells, suppressing DNA synthesis and cellular growth, whereas the MTX loaded into CS-NPs induced both cytostatic and cytotoxic effects [45,46]. Finally, we showed that the LMP effect participated slightly in the mechanism involved in MTX-CS-NPs toxicity in HeLa cells, but not in MCF-7 cells. The LMP induced in HeLa cells by high concentrations of NPs suggests that the lysosomal damage might play some role in the resulting apoptotic effects of MTX-CS-NPs. It was reported that the LMP effect leads to the translocation of lysosomal hydrolases to the rest of the cell, which frequently mediates apoptosis by inducing mitochondrial structural dysfunction [46]. These results indicated that the damage of lysosomal integrity and the early mitochondrial injury (corroborated by the higher sensitivity of MTT assay for detecting NP cytotoxicity) might also support the greater susceptibility of HeLa cells to the toxic effects of MTX.

The assessment of the hemocompatibility of a nanocarrier is indispensable for frequent intravenous dosing. The incorporation of MTX into the NPs was found to increase their hemolytic potential. However, when tested under the same conditions as the NP formulations, free MTX did not induce any undesirable response. Therefore, the main source of hemolysis might be the effects that the drug moiety produces on the NP surface or when encapsulated on it. Indeed, it was recently reported that MTX incorporated in liposomal formulations displayed higher hemoreactivity than its free solution [47]. The agglutination induced by the NPs at the highest concentration tested may be caused by increased binding of the NPs to the erythrocyte membrane, which might deformed cells and hence decrease the repulsion among them [48].

In our previous study [17], we showed the high efficiency of the amphiphile 77KL at disrupting cell membranes within the pH range characteristic of late endosomes. Therefore, the rationale behind assessing the membrane-lytic behavior of the NPs was to establish the ability of NPs containing this amphiphile to promote triggered release of entrapped molecules in a pH-dependent fashion. The enhanced hemolysis induced by NPs at acidic pH might be due to the increasing protonation state of the carboxylic group of 77KL in this condition. The protonation of the 77KL molecule makes it non-ionic and enhances its hydrophobicity, which would increase binding to the membrane and, thus, its lysis. The rather unexpected greater membrane-lytic activity of MTX-CS-NPs could be attributed to a competitive effect between MTX and 77KL molecules for binding to the positive NP surface. Both structures were negative charged and, thus, MTX molecules could induce faster release of 77KL molecules from the NP surface, which would result in increased hemolysis.

The membrane-lytic activity of the NPs in an acidic environment might facilitate escape from the endocytotic pathway to lysosomes, and allow efficient intracellular drug delivery to the cell cytosol. To corroborate this pH-sensitive activity of the NPs at intracellular level, we used calcein as an endosomal tracer molecule, which is internalized by the cell through endocytosis and is used to monitor the stability of endosomes following NP uptake [35]. In the absence of NPs, endosomal compartmentalization of calcein was observed, which indicates that the endosome membranes were not damaged [35]. In contrast, the CS-NPs induced efficient release of endocytosed material into the cytoplasm. On the basis of these experiments, we conclude that the NPs deliver calcein to the cytosol of cells by co-endocytosis of this dye and NPs, followed by NP-induced disruption of endosomes and escape of the dye into the cytosol. The cellular uptake of CS-NPs seems to occur by adsorptive endocytosis, as the uptake of similar NPs was previously reported to occur predominantly by adsorptive endocytosis in A549 cells [49] as well as in the HeLa cell line [15].

## 5. Conclusions

In this study, MTX-loaded CS-NPs have been successfully formulated as an intracellular delivery system for improved antitumor activity. The inclusion of the surfactant 77KL on the NP formulations clearly gives them pH-sensitive membrane-lytic behavior. This facilitates cytosolic delivery of the fluorescent endosomal tracer calcein, and consequently of the encapsulated drug, through endosomal membrane lysis. Furthermore, the NPs showed high encapsulation efficiency, accelerated release of MTX at a decreasing pH from 7.4 to 5.4, acceptable hemocompatibility and enhanced cytotoxicity on HeLa and MCF-7 tumor cell lines in comparison to free MTX. Another advantage of MTX-CS-NPs was found to be their greater cytotoxic activity around tumor extracellular  $pH_e$  compared to that at physiological pH. The combination of the physicochemical characteristics and pH-sensitivity of the NPs resulted in superior cytotoxicity of the entrapped drug, together with generally greater cell cycle arrest and a higher apoptotic response. Based on the overall results, the combined mechanisms of pH-triggered release and cytotoxicity, together with the specific ability to lyse the endosomal membrane after cell internalization, makes MTX-CS-NPs containing the lysine-based surfactant 77KL a beneficial approach that provides increased anticancer efficacy at the tumor site. However, further *in vivo* studies must be conducted in this field to prove the hypothesis.

### Conflict of interest statement

The authors state that they have no conflict of interest.

### Acknowledgments

This research was supported by Projects CTQ2009-14151-C02-02 and CTQ2009-14151-C02-01 of the *Ministerio de Ciencia e Innovación* (Spain). Daniele Rubert Nogueira holds a PhD grant from MAEC-AECID (Spain).

## References

- [1] Bao H, Li L, Zhang H. Influence of cetyltrimethylammonium bromide on physicochemical properties and microstructures of chitosan-TPP nanoparticles in aqueous solutions. *J Coll Interface Sci* 2008;328:270-277.
- [2] Fan W, Yan W, Xu Z, Ni H. Formation mechanism of monodisperse, low molecular weight chitosan nanoparticles by ionic gelation technique. *Colloids Surf B Biointerfaces* 2012;90:21-27.
- [3] Vila A, Sánchez A, Janes K, Behrens I, Kissel T, Jato JLV, et al. Low molecular weight chitosan nanoparticles as new carriers for nasal vaccine delivery in mice. *Eur J Pharm Biopharm* 2004;57:123-131.
- [4] Mehrotra A, Nagrawal RC, Pandit JK. Lomustine loaded chitosan nanoparticles: characterization and in-vitro cytotoxicity on human cancer cell line L132. *Chem Pharm Bull* 2011;59:315-320.
- [5] Trapani A, Denora N, Iacobellis G, Sitterberg J, Bakowsky U, Kissel T. Methotrexate-loaded chitosan and glycolchitosan-based nanoparticles: a promising strategy for the administration of the anticancer drug to brain tumors. *AAPS Pharm. Sci Tech* 2011;12:1302-1311.
- [6] Calvo P, Remuñan-López C, Vila-Jato JL, Alonso MJ. Chitosan and chitosan/ethylene oxide-propylene oxide block copolymer nanoparticles as novel carriers for proteins and vaccines. *Pharm Res* 1997;14:1431-1436.
- [7] Gan Q, Wang T, Cochrane C, McCarron P. Modulation of surface charge, particle size and morphological properties of chitosan-TPP nanoparticles intended for gene delivery. *Colloids Surf B Biointerfaces* 2005;44:65-73.
- [8] Berger J, Reist M, Mayer JM, Felt O, Peppas NA, Gurny R. Structure and interactions in covalently and ionically crosslinked chitosan hydrogels for biomedical applications. *Eur J Pharm Biopharm* 2004;57:19-34.
- [9] Duthie SJ. Folic-acid-mediated inhibition of human colon-cancer cell growth. *Nutrition* 2001;17:736-737.
- [10] Yoon S-A, Choi JR, Kim J-O, Shin J-Y, Zhang X, Kang J-H. Influence of reduced folate carrier and dihydrofolate reductase genes on methotrexate-induced cytotoxicity. *Cancer Res Treat* 2010;42:163-171.

- [11] Banerjee D, Mayer-Kuckuk P, Capiiaux G, Budak-Alpdogan T, Gorlick R, Bertino JR. Novel aspects of resistance to drugs targeted to dihydrofolate reductase and thymidylate synthase. *Biochim Biophys Acta* 2002;1587:164-173.
- [12] Das M, Sahoo SK. Epithelial cell adhesion molecule targeted nutlin-3a loaded immunonanoparticles for cancer therapy. *Acta Biomater* 2011;7:355-369.
- [13] Saboktakin MR, Tabatabaie RM, Maharramov A, Ramazanov MA. Synthesis and characterization of pH-dependent glycol chitosan and dextran sulfate nanoparticles for effective brain cancer treatment. *Int J Biol Macromol* 2011;49:747-751.
- [14] Wu P, He X, Wang K, Tan W, He C, Zheng M. A novel methotrexate delivery system based on chitosan-methotrexate covalently conjugated nanoparticles. *J Biomed Nanotechnol* 2009;5:557-564.
- [15] Park JS, Han TH, Lee KY, Han SS, Hwang JJ, Moon DH, et al. *N*-acetyl histidine-conjugated glycol chitosan self-assembled nanoparticles for intracytoplasmic delivery of drugs: endocytosis, exocytosis and drug release. *J Control Release* 2006;115:37-45.
- [16] Bae Y, Nishiyama N, Fukushima S, Koyama H, Yasuhiro M, Kataoka K. Preparation and biological characterization of polymeric micelle drug carriers with intracellular pH-triggered drug release property: tumor permeability, controlled subcellular drug distribution, and enhanced *in vivo* antitumor efficacy. *Bioconj Chem* 2005;16:122-130.
- [17] Nogueira DR, Mitjans M, Infante MR, Vinardell MP. The role of counterions in the membrane-disruptive properties of pH-sensitive lysine-based surfactants. *Acta Biomater* 2011;7:2846-2856.
- [18] Nogueira DR, Mitjans M, Morán MC, Pérez L, Vinardell MP. Membrane-destabilizing activity of pH-responsive cationic lysine-based surfactants: role of charge position and alkyl chain length. *Amino Acids* 2012;43:1203-1215.
- [19] Colomer A, Pinazo A, Garcia T, Mitjans M, Vinardell P, Infante MR, Martínez V, Pérez L. pH sensitive surfactants from lysine: assessment of their cytotoxicity and environmental behavior. *Langmuir* 2012;28:5900-5912.
- [20] Vives MA, Infante MR, Gracia E, Selve C, Maugras M, Vinardell MP. Erythrocyte hemolysis and shape changes induce by new lysine-derivate surfactants. *Chem Biol Interact* 1999;118:1-18.
- [21] Nogueira DR, Mitjans M, Infante MR, Vinardell MP. Comparative sensitivity of tumor and non-tumor cell lines as a reliable approach for *in vitro* cytotoxicity screening of lysine-based surfactants with potential pharmaceutical applications. *Int J Pharm* 2011;420:51-58.

- [22] Tavano L, Muzzalupo R, Trombino S, Cassano R, Pingitore A, Picci N. Effect of formulations variables on the in vitro percutaneous permeation of sodium diclofenac from new vesicular systems obtained from Pluronic triblock copolymers. *Colloids Surf B Biointerfaces* 2010;79:227-234.
- [23] Na K, Lee ES, Bae YH. Adriamycin loaded pullulan acetate/sulfonamide conjugate nanoparticles responding to tumor pH: pH-dependent cell interaction, internalization and cytotoxicity in vitro. *J Control Release* 2003;87:3-13.
- [24] Mosmann T. Rapid colorimetric assay to cellular growth and survival: application to proliferation and cytotoxicity assays. *J Immunol Methods* 1983;65:55-63.
- [25] Venkatesan P, Puvvada N, Dash R, Kumar BNP, Sarkar D, Azab B, et al. The potential of celecoxib-loaded hydroxyapatite-chitosan nanocomposite for the treatment of colon cancer. *Biomaterials* 2011;32:3794-3806.
- [26] Nogueira DR, Morán MC, Mitjans M, Martínez V, Pérez L, Vinardell MP. New cationic nanovesicular systems containing lysine-based surfactants for topical administration: toxicity assessment using representative skin cell lines. *Eur J Pharm Biopharm* 2012. *In press*. DOI: 10.1016/j.ejpb.2012.09.007.
- [27] Borenfreund E, Puerner JA. Toxicity determined in vitro by morphological alterations and neutral red absorption. *Toxicol Lett* 1985;24:119-124.
- [28] Fröhlich E, Meindl C, Roblegg E, Griesbacher A, Pieber TR. Cytotoxicity of nanoparticles is influenced by size, proliferation and embryonic origin of the cells used for testing. *Nanotoxicology* 2012;6:424-439.
- [29] Yang H, Liu C, Yang D, Zhang H, Xi Z. Comparative study of cytotoxicity, oxidative stress and genotoxicity induced by four typical nanomaterials: the role of particle size, shape and composition. *J Appl Toxicol* 2009;29:69-78.
- [30] Monteiro-Riviere NA, Inman AO, Zhang LW. Limitations and relative utility of screening assays to assess engineered nanoparticle toxicity in a human cell line. *Toxicol Appl Pharmacol* 2009;234:222-235.
- [31] Squier MKT, Cohen JJ. Standard quantitative assays for apoptosis. *Mol Biotechnol* 2001;19:305-312.
- [32] Sohaebuddin S, Thevenot PT, Baker D, Eaton JW, Tang L. Nanomaterial cytotoxicity is composition, size, and cell type dependent. *Particle Fibre Toxicol* 2010;7:22.
- [33] Wang X-L, Ramusovis S, Nguyen T, Lu Z-R. Novel polymerizable surfactants with pH-sensitive amphiphilicity and cell membrane disruption for efficient siRNA delivery. *Bioconj Chem* 2007;18:2169-2177.

- [34] Akagi T, Kim H, Akashi M. pH-dependent disruption of erythrocyte membrane by amphiphilic poly(amino acid) nanoparticles. *J Biomater Sci* 2010;21:315-328.
- [35] Hu Y, Litwin T, Nagaraja AR, Kwong B, Katz J, Watson N, et al. Cytosolic delivery of membrane-impermeable molecules in dendritic cells using pH-responsive core-shell nanoparticles. *Nano Lett* 2007;7:3056-3064.
- [36] Mao S, Sun W, Kissel T. Chitosan-based formulations for delivery of DNA and siRNA. *Adv Drug Deliv Rev* 2010;62:12-27.
- [37] Gan Q, Wang T. Chitosan nanoparticle as protein delivery carrier – Systematic examination of fabrication conditions for efficient loading and release. *Colloids Surf B Biointerfaces* 2007;59:24-34.
- [38] Ojogun VA, Lehmler H-J, Knutson BL. Cationic-anionic vesicle templating from fluorocarbon/fluorocarbon and hydrocarbon/fluorocarbon surfactants. *J Coll Interf Sci* 2009;338:82-91.
- [39] Gao F, Cai Y, Zhou J, Xie X, Ouyang W, Zhang Y, et al. Pullulan acetate coated magnetic nanoparticles for hyperthermia: preparation, characterization and *in vitro* experiments. *Nano Res* 2010;3:23-31.
- [40] Jingou J, Shilei H, Weiqi L, Danjun W, Tengfei W, Yi X. Preparation, characterization of hydrophilic and hydrophobic drug in combine loaded chitosan/cyclodextrin nanoparticles and *in vitro* release study. *Colloids Surf B Biointerfaces* 2011;83:103-107.
- [41] Kusnetsova N, Kandyba A, Vostrov I, Kadykov V, Gaenko G, Molotkovsky J, et al. Liposomes loaded with lipophilic prodrugs of methotrexate and melphalan as convenient drug delivery vehicles. *J Drug Del Sci Tech* 2009;19:51-59.
- [42] Mei L, Zhang Y, Zheng Y, Tian G, Song C, Yang D, et al. A novel docetaxel-loaded poly ( $\epsilon$ -caprolactone)/pluronic F68 nanoparticle overcoming multidrug resistance for breast cancer treatment. *Nanoscale Res Lett* 2009;4:1530-1539.
- [43] Brigger I, Dubernet C, Couvreur P. Nanoparticles in cancer therapy and diagnosis. *Adv Drug Deliv Rev* 2002;54:631-651.
- [44] Qiu L, Zhang L, Zheng C, Wang R. Improving physicochemical properties of doxorubicin cytotoxicity of novel polymeric micelles by poly ( $\epsilon$ -caprolactone) segments. *J Pharm Sci* 2011;100:2430-2442.
- [45] Sánchez-del-Campo L, Montenegro MF, Cabezas-Herrera J, Rodríguez-López JN. The critical role of alpha-folate receptor in the resistance of melanoma to methotrexate. *Pigment Cell Melanoma Res* 2009;22:588-600.

- [46] Joanitti GA, Azevedo RB, Freitas SM. Apoptosis and lysosome membrane permeabilization induction on breast cancer cells by an anticarcinogenic Bowman-Birk protease inhibitor from *Vigna unguiculata* seeds. *Cancer Lett* 2010;293:73-81.
- [47] Kuznetsova NR, Sevrin C, Lespineux D, Bovin NV, Vodovozova EL, Mészáros T, et al. Hemocompatibility of liposomes loaded with lipophilic prodrugs of methotrexate and melphalan in the lipid bilayer. *J Control Release* 2012;160:394-400.
- [48] Li S-Q, Zhu R-R, Zhu H, Xue M, Sun X-Y, Yao S-D, et al. Nanotoxicity of TiO<sub>2</sub> nanoparticles to erythrocyte in vitro. *Food Chem Toxicol* 2008;46:3623-3631.
- [49] Huang M, Ma Z, Khor E, Lim L-Y. Uptake of FITC-chitosan nanoparticles by A549 cells. *Pharm Res* 2002;19:1488-1494.

## Figure captions:

**Fig. 1.** pH-dependent *in vitro* cumulative release of MTX from NPs in PBS buffer at pH 7.4, 6.5 and 5.4. Results are expressed as the mean  $\pm$  SE of three independent experiments. Statistical analyses were performed using ANOVA followed by Tukey's multiple comparison test. <sup>a</sup> Significantly different from PBS pH 7.4 ( $p < 0.05$ ) and <sup>b</sup> significantly different from PBS pH 6.5 ( $p < 0.05$ ).

**Fig. 2.** The effect of MTX-CS-NPs or free MTX concentration and viability assay (MTT and NRU) on the survival rates of (a) HaCaT, (b) HeLa and (c) MCF-7 cell lines. Data are expressed as the mean of three independent experiments  $\pm$  SE. Statistical analyses were performed using ANOVA followed by Tukey's multiple comparison test. <sup>a</sup> Significantly different from HaCaT cells ( $p < 0.05$ ) and <sup>b</sup> significantly different from MCF-7 cells ( $p < 0.05$ ). \*  $p < 0.05$  and \*\*  $p < 0.005$  denote significant differences from free MTX.

**Fig. 3.** Cytotoxicity of MTX-CS-NPs and free MTX on HeLa and MCF-7 tumor cell lines. (A) Time-dependent cytotoxicity of MTX-CS-NPs and free MTX at the 0.001-50  $\mu\text{g/ml}$  concentration range in tumor HeLa and MCF-7 cells, as determined by a MTT assay. (B) pH-dependent cytotoxicity of MTX-CS-NPs and free MTX against HeLa and MCF-7 cells after 4 and 24 h incubation, as determined by a MTT assay. Data are expressed as the mean of three independent experiments  $\pm$  SE. Statistical analyses were performed using ANOVA followed by Tukey's multiple comparison test. \*  $p < 0.05$  and \*\*  $p < 0.005$  denote significant differences from the cytotoxic effects at pH 7.4.

**Fig. 4.** Effect of MTX-CS-NPs and free MTX on apoptosis of (a) HeLa cells and (b) MCF-7 cells determined by fluorescence microscopy after AO/BE staining. Results are expressed as the percentage of viable, apoptotic and necrotic cells after 24 h treatment with 1, 10 or 50  $\mu\text{g/ml}$  of MTX-CS-NPs or free MTX. Fluorescent micrographs of HeLa cells: (c) untreated control cells, (d) 50  $\mu\text{g/ml}$  free MTX, (e) 50  $\mu\text{g/ml}$  MTX-CS-NPs and of MCF-7 cells: (f) untreated control cells, (g) 50  $\mu\text{g/ml}$  free MTX, (h) 50  $\mu\text{g/ml}$  MTX-CS-NPs. Legends: (►) typical live nuclei, (▼) chromatin condensation (early apoptosis), (▲) blebbing and nuclear margination (early to moderate apoptosis), (\*) necrosis, (\*\*) late apoptosis. Statistical analyses were performed using ANOVA followed by Dunnett's or Tukey's multiple comparison test. \*  $p < 0.05$  and \*\*  $p < 0.005$  denote significant differences from untreated control cells. <sup>a</sup> Significantly different from free MTX ( $p < 0.05$ ).

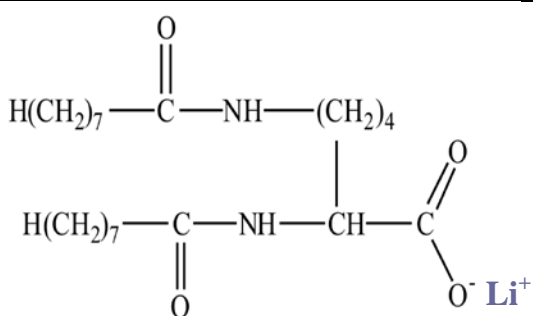
**Fig. 5.** Cell-cycle analysis of (a) HeLa and (b) MCF-7 cells following 24 h treatment with 1, 10 or 50  $\mu\text{g/ml}$  of MTX-CS-NPs or free MTX. Results are expressed as the mean  $\pm$  SE of three independent experiments, performed in duplicate. Statistical analyses were performed using ANOVA followed by Dunnett's or Tukey's multiple comparison test. \*  $p < 0.05$ , \*\*  $p < 0.005$  denote significant differences from untreated control cells. <sup>a</sup> Significantly different from free MTX ( $p < 0.05$ ).

**Fig. 6.** Assessment of MTX-CS-NPs and free MTX effects on lysosomal membrane permeabilization (LMP) in HeLa and MCF-7 cells as visualized via AO staining. In untreated control cells, lysosomes can be seen as red-orange granules and cytoplasm has a diffuse green fluorescence. In cells with lysosomal membrane damage (HeLa cells treated with 50  $\mu\text{g}/\text{ml}$  MTX-CS-NPs), lysosomes exhibit a shift from red-orange to a yellow-green fluorescent color.

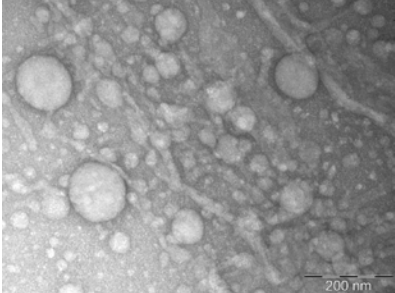
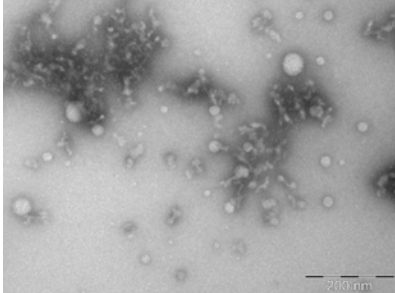
**Fig. 7.** Hemocompatibility of unloaded-CS-NPs and MTX-CS-NPs. (A) Percentage of hemolysis caused by NPs after 10 and 60 min of incubation with rat erythrocytes. Each value represents the mean  $\pm$  SE of three experiments. (B) Agglutination of rat erythrocytes observed by phase microscopy after 1h of incubation with 500  $\mu\text{g}/\text{ml}$  of NPs.

**Fig. 8.** (A) pH-sensitive membrane-lytic activity of unloaded-CS-NPs (with or without 77KL) and MTX-CS-NPs. NP-induced hemoglobin release from rat erythrocytes was expressed as a function of pH, concentration and incubation time. Results are expressed as the mean  $\pm$  SE of three independent experiments. Statistical analyses were performed using ANOVA followed by Tukey's multiple comparison test. <sup>a</sup> Significantly different from pH 7.4 ( $p < 0.05$ ) and <sup>b</sup> significantly different from pH 6.5 ( $p < 0.05$ ). (B) Fluorescence microscopy images of HeLa cells showing the subcellular distribution of calcein fluorescence. The cells were treated with 1 mg/ml calcein (control); both 1 mg/ml calcein and 250 or 500  $\mu\text{g}/\text{ml}$  of unloaded-CS-NPs or 25 or 50  $\mu\text{g}/\text{ml}$  of MTX-CS-NPs. Images were acquired at 3 h after 1 h of uptake.

**Table 1.** Physicochemical properties of the anionic lysine-based surfactant 77KL.

Chemical structure	Molecular weight	405.6 g/mol
	Critical micellar concentration (CMC)	$2.9 \times 10^3 \mu\text{g/ml}$
	pKa	6.2
	Number of alkyl chains	2
	Length of alkyl chain	C8

**Table 2.** Characterization properties of the nanoparticles.

	Unloaded-CS-NPs	MTX-CS-NPs
	Hydrodynamic size (nm) $\pm$ SE <sup>a</sup>	
t = 0 h water	350.47 $\pm$ 13.31	301.17 $\pm$ 8.96
t = 0 h DMEM 5% FBS	579.40 $\pm$ 18.71/ 17.39 $\pm$ 0.45 <sup>c</sup>	483.50 $\pm$ 45.03/ 14.80 $\pm$ 0.78 <sup>c</sup>
t = 24 h water <sup>b</sup>	403.53 $\pm$ 13.23	312.57 $\pm$ 9.71
t = 24 h DMEM 5% FBS <sup>b</sup>	108.41 $\pm$ 14.42/ 723.15 $\pm$ 32.15 <sup>c</sup>	147.73 $\pm$ 1.83
	PDI $\pm$ SE <sup>a</sup>	
t = 0 h water	0.269 $\pm$ 0.009	0.257 $\pm$ 0.008
t = 0 h DMEM 5% FBS	1.00 $\pm$ 0.001	0.680 $\pm$ 0.011
t = 24 h water <sup>b</sup>	0.260 $\pm$ 0.018	0.269 $\pm$ 0.005
t = 24 h DMEM 5% FBS <sup>b</sup>	0.517 $\pm$ 0.087	0.431 $\pm$ 0.029
	ZP (mV) $\pm$ SE <sup>a</sup>	
t = 0 h water	30.07 $\pm$ 1.18	26.87 $\pm$ 0.90
t = 0 h DMEM 5% FBS	-4.41 $\pm$ 0.35	-4.74 $\pm$ 0.29
	TEM diameter (nm)	
t = 0 h water	20 - 140	20 - 60
TEM images <sup>d</sup>		

<sup>a</sup> Mean of three experiments  $\pm$  SE.

<sup>b</sup> Incubated under cell culture conditions: 37°C, 5% CO<sub>2</sub>.

<sup>c</sup> Predominant size is indicated first.

<sup>d</sup> Scale bars = 200 nm

**Table 3.** Cytotoxicity expressed as IC<sub>50</sub> values of free MTX, unloaded-CS-NPs and MTX-loaded-CS-NPs in HeLa, MCF-7 and HaCaT cell lines.

Cytotoxicity assay – 24 h treatment - IC <sub>50</sub> ± SE (µg/ml)			
Cell line	MTT	NRU	LDH
Free MTX			
HeLa	> 50	> 50	> 50
MCF-7	> 50	> 50	> 50
HaCaT	> 50	> 50	> 50
MTX-CS-NPs			
HeLa	4.37 ± 0.37	17.69 ± 0.14	> 50
MCF-7	34.72 ± 6.23	35.35 ± 5.38	> 50
HaCaT	> 50	> 50	> 50
Unloaded-CS-NPs			
HeLa	260.39 ± 54.32	> 500	> 500
MCF-7	> 500	> 500	> 500
HaCaT	> 500	> 500	> 500
Time-dependent antitumoral activity - IC <sub>50</sub> ± SE (µg/ml) – MTT assay			
pH 7.4			
	4 h	24 h	48 h
Free MTX			
HeLa	> 50	> 50	0.0089 ± 0.12
MCF-7	> 50	> 50	19.13 ± 2.37
MTX-CS-NPs			
HeLa	42.93 ± 2.37	4.37 ± 0.37	0.0098 ± 0.05
MCF-7	> 50	34.72 ± 6.23	8.76 ± 1.07
pH 6.6			
Free MTX			
HeLa	> 50	> 50	-
MCF-7	> 50	> 50	-
MTX-CS-NPs			
HeLa	21.86 ± 1.98	6.76 ± 2.54	-
MCF-7	33.09 ± 2.31	28.97 ± 1,74	-

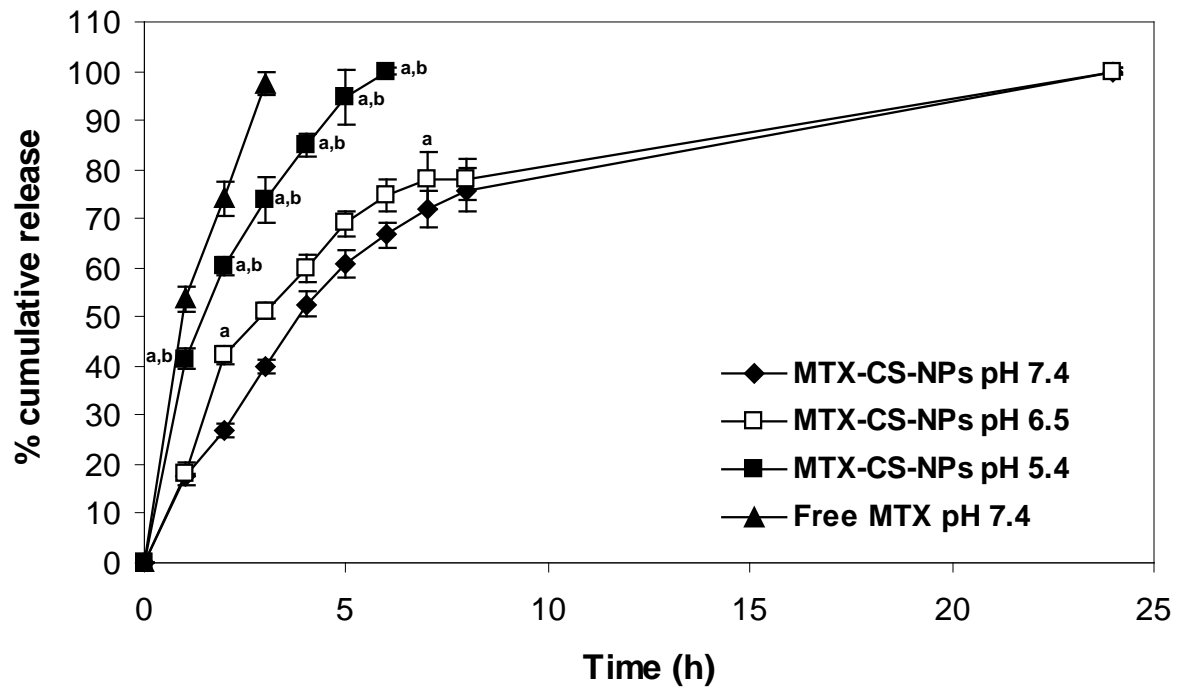


Fig. 1

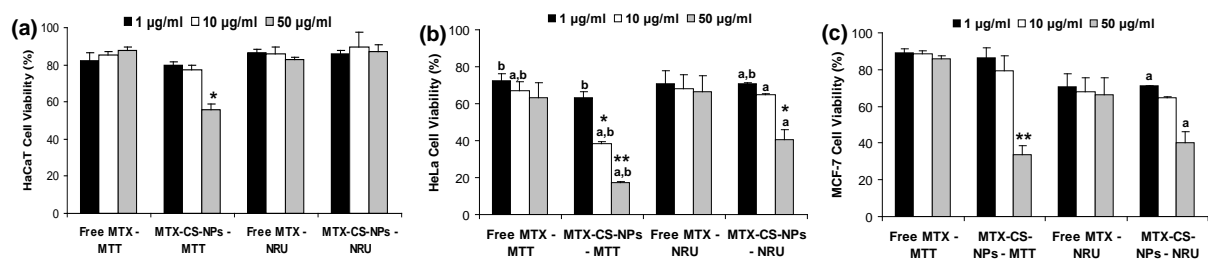


Fig. 2

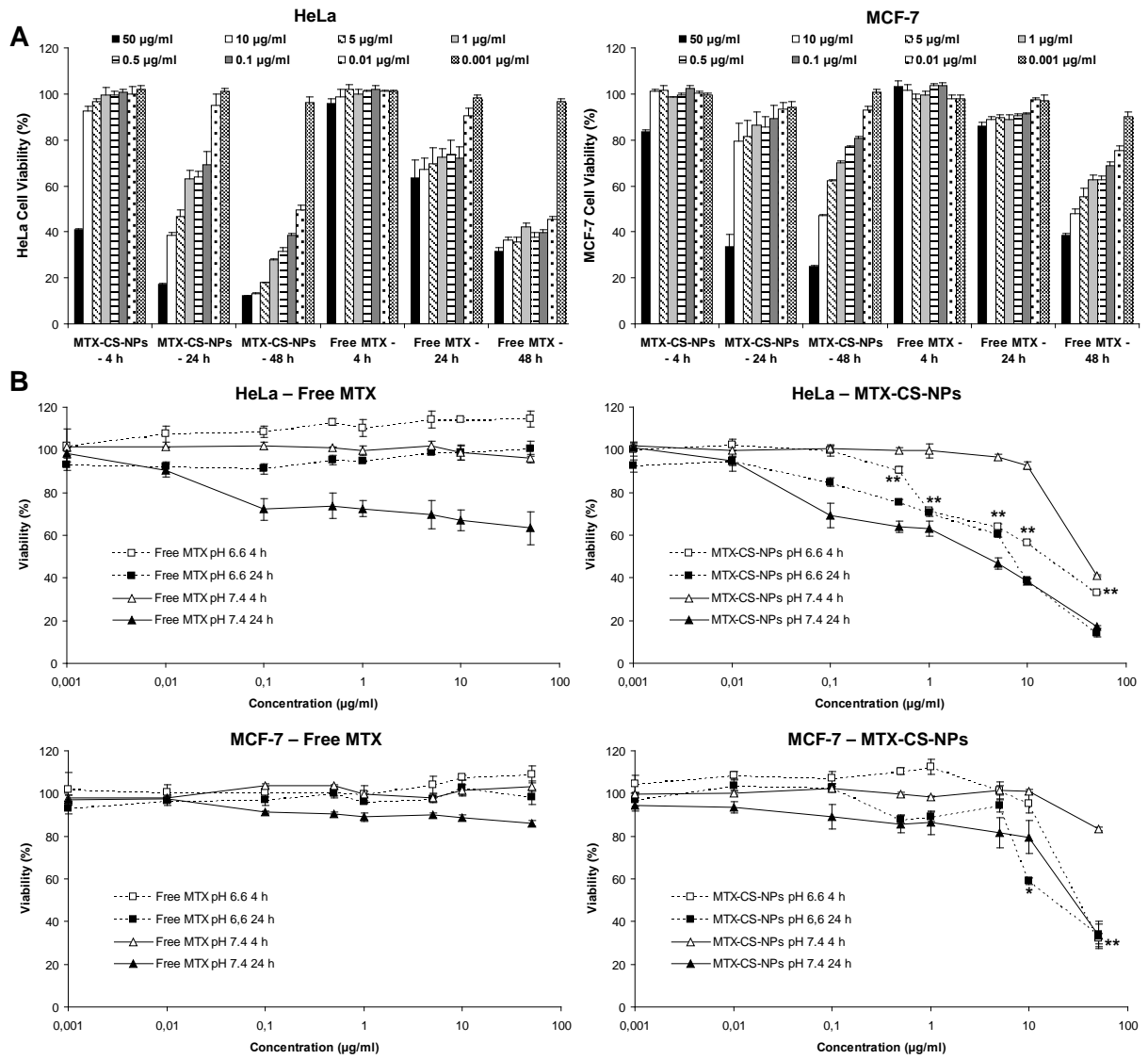


Fig. 3

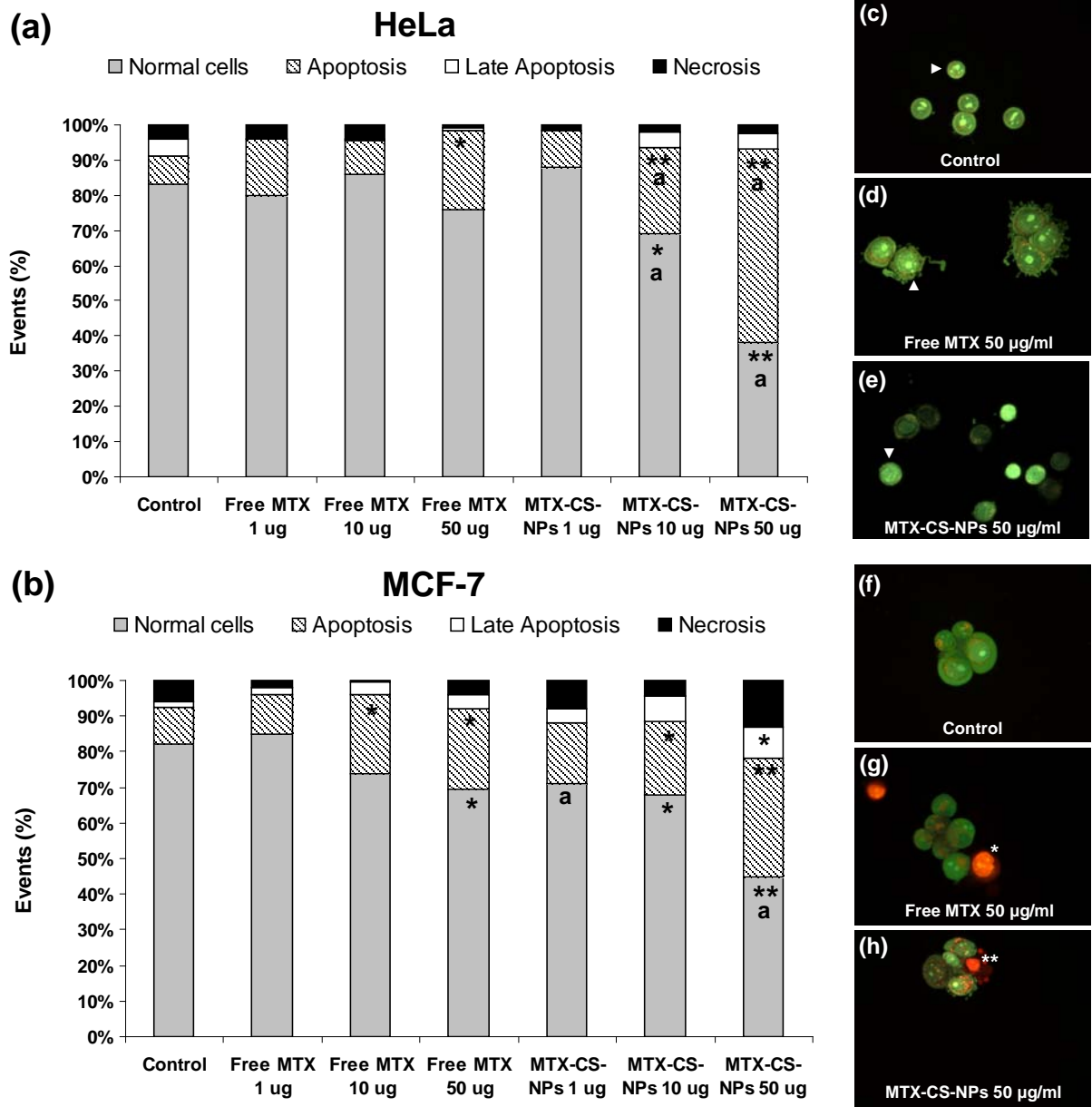


Fig. 4

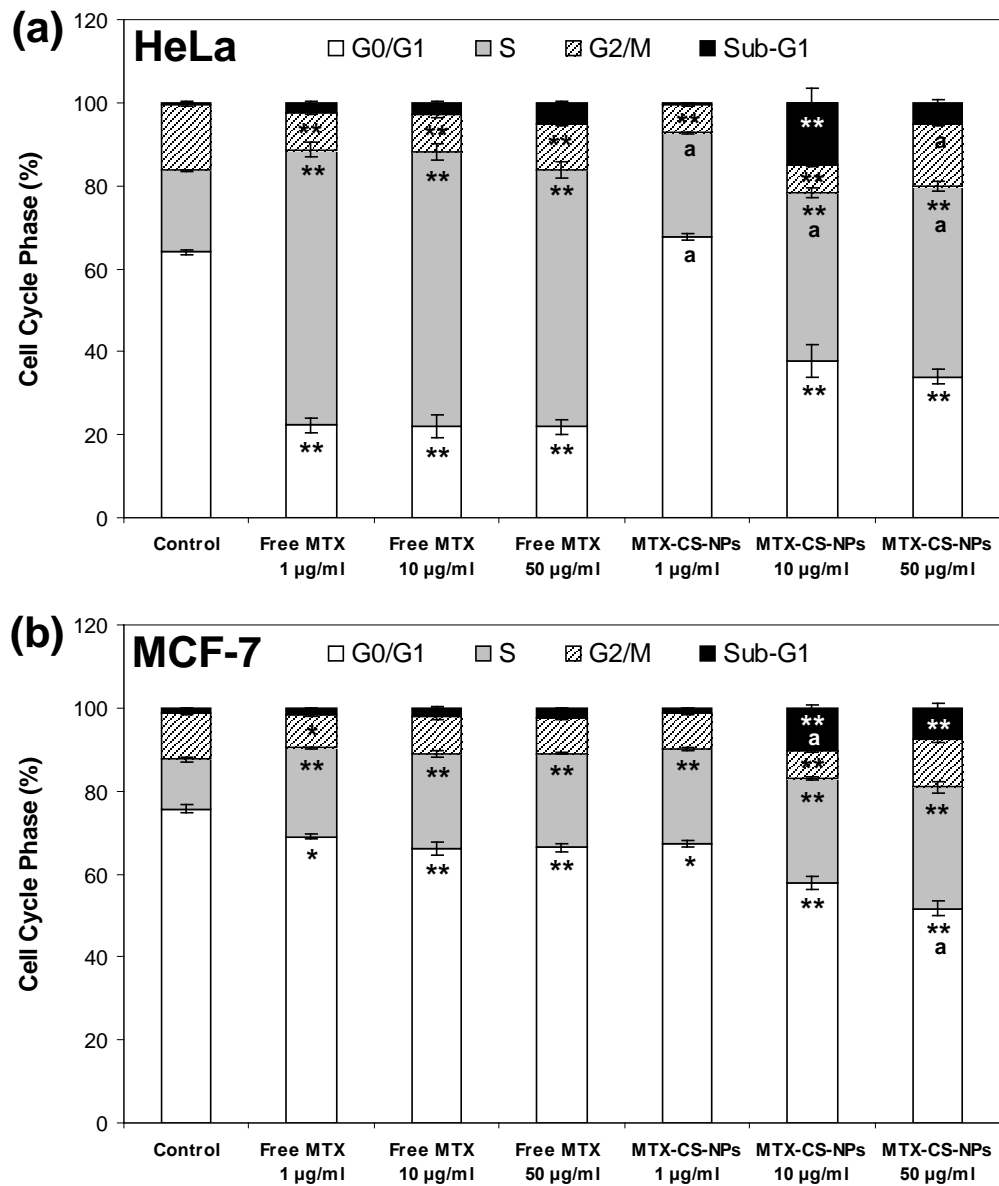


Fig. 5

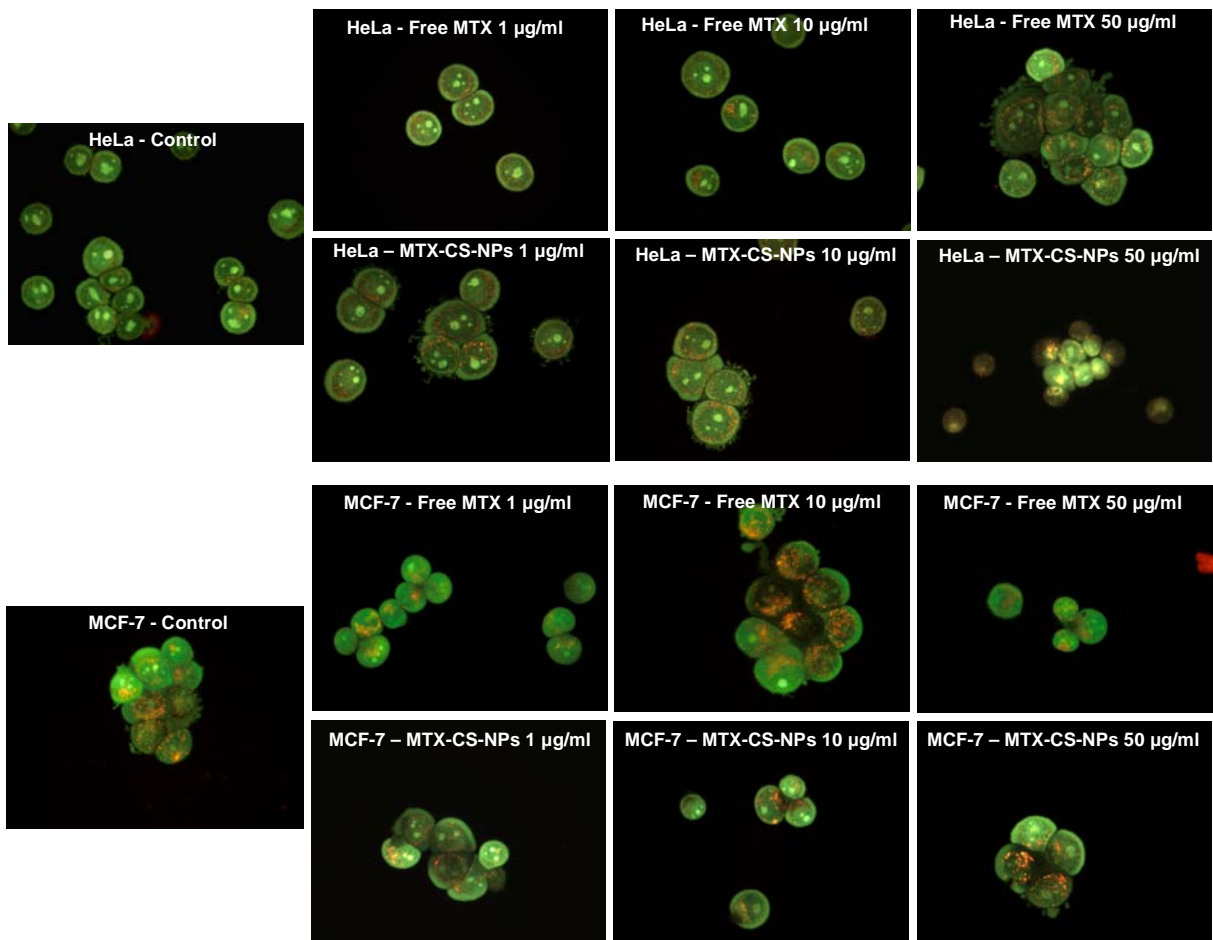


Fig. 6

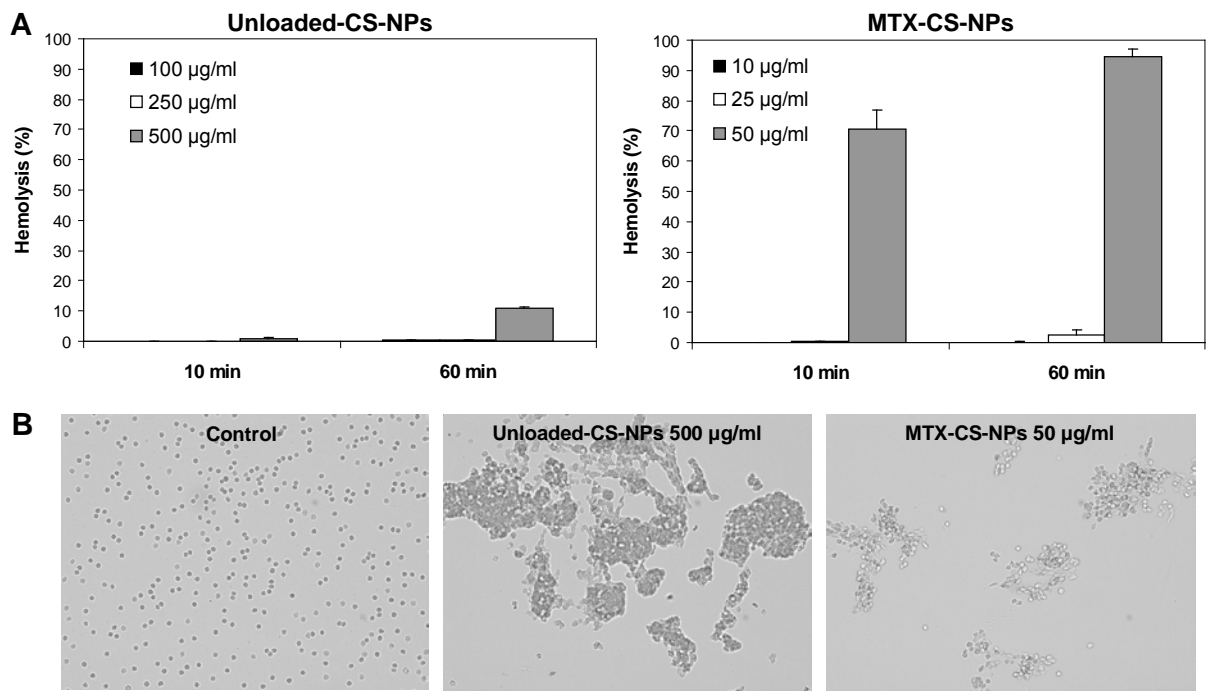


Fig. 7

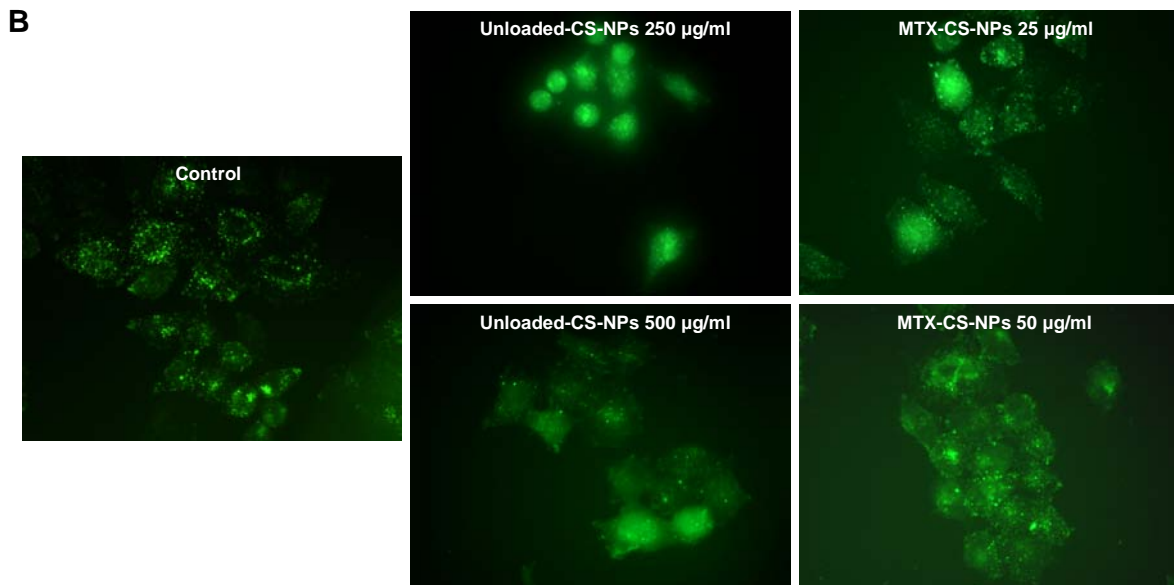
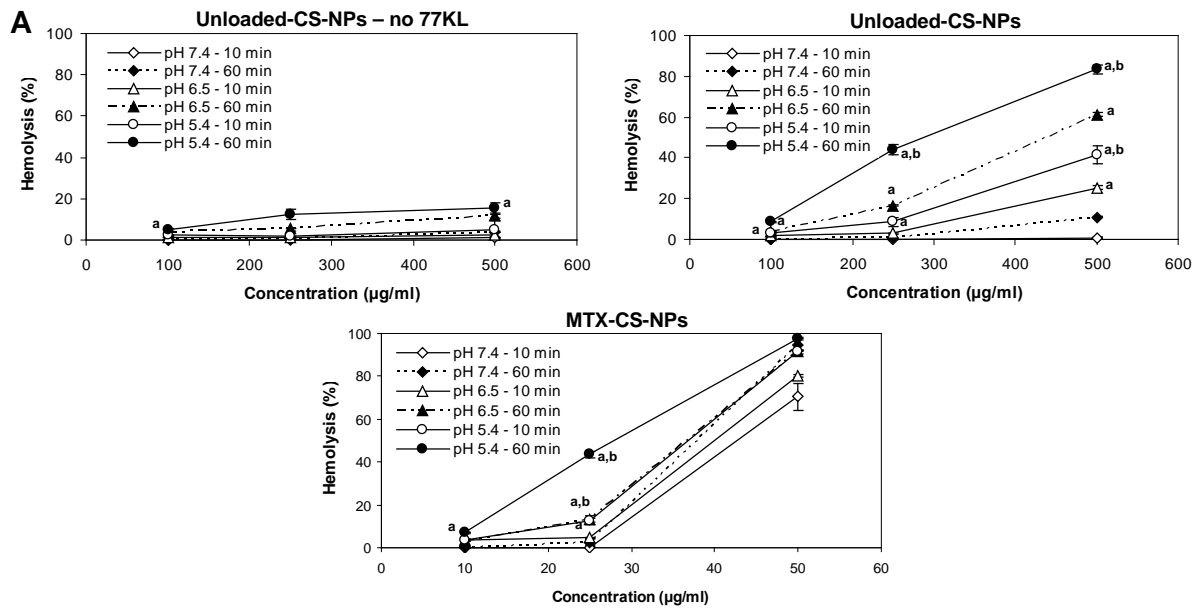


Fig. 8